

## A comparison of observations and model simulations of NO<sub>x</sub>/NO<sub>y</sub> in the lower stratosphere

R. S. Gao,<sup>1,2</sup> D. W. Fahey<sup>1,2</sup>, L. A. Del Negro<sup>1,2,3</sup>, S. G. Donnelly<sup>1,2</sup>, E. R. Keim<sup>4</sup>, J. A. Neuman<sup>1,2</sup>, E. Teverovskaia<sup>1,2</sup>, P. O. Wennberg<sup>5</sup>, T. F. Hanisco<sup>6</sup>, E. J. Lanzendorf<sup>6</sup>, M. H. Proffitt<sup>1,2</sup>, J. J. Margitan<sup>7</sup>, J. C. Wilson<sup>8</sup>, J. W. Elkins<sup>9</sup>, R. M. Stimpfle<sup>6</sup>, R. C. Cohen<sup>10</sup>, C. T. McElroy<sup>11</sup>, T. P. Bui<sup>12</sup>, R. J. Salawitch<sup>7</sup>, S. S. Brown<sup>1,2</sup>, A. R. Ravishankara<sup>1,2,3</sup>, R. W. Portmann<sup>1</sup>, M. K. W. Ko<sup>13</sup>, D. K. Weisenstein<sup>13</sup>, and P. A. Newman<sup>14</sup>

**Abstract.** Extensive airborne measurements of the reactive nitrogen reservoir (NO<sub>y</sub>) and its component nitric oxide (NO) have been made in the lower stratosphere. Box model simulations that are constrained by observations of radical and long-lived species and which include heterogeneous chemistry systematically underpredict the NO<sub>x</sub> (= NO + NO<sub>2</sub>) to NO<sub>y</sub> ratio. The model agreement is substantially improved if newly measured rate coefficients for the OH + NO<sub>2</sub> and OH + HNO<sub>3</sub> reactions are used. When included in 2-D models, the new rate coefficients significantly increase the calculated ozone loss due to NO<sub>x</sub> and modestly change the calculated ozone abundances in the lower stratosphere. Ozone changes associated with the emissions of a fleet of supersonic aircraft are also altered.

high latitude lower stratosphere during summer. This data set provides a unique opportunity to test our understanding of the gas-phase chemistry linking NO<sub>x</sub> and nitric acid (HNO<sub>3</sub>), which is generally the most abundant NO<sub>y</sub> species. Because the continuous daylight present at summer high latitudes limits the heterogeneous production of HNO<sub>3</sub> by N<sub>2</sub>O<sub>5</sub> hydrolysis, gas-phase reactions primarily control the balance between NO<sub>x</sub> and NO<sub>y</sub>. Outside summer polar regions, the N<sub>2</sub>O<sub>5</sub> hydrolysis reaction occurring on stratospheric sulfate aerosols is a more important sink of NO<sub>x</sub> [*cf. Fahey et al., 1993*], particularly in the lower stratosphere during winter when heterogeneous pathways account for most of the HNO<sub>3</sub> production [*cf. Gao et al., 1997*].

### Introduction

Understanding the mechanisms controlling the abundance of NO<sub>y</sub> and its partitioning into component species is an essential requirement for understanding the stratospheric ozone (O<sub>3</sub>) layer. Reactions involving NO<sub>x</sub> form a catalytic O<sub>3</sub> destruction cycle and also moderate O<sub>3</sub> loss due to other cycles involving reactive hydrogen (HO<sub>x</sub>) and halogens (ClO<sub>x</sub>-BrO<sub>x</sub>) [*cf. Wennberg et al., 1994*]. The partitioning of the NO<sub>y</sub> reservoir between NO<sub>x</sub> and other component species involves gas-phase and heterogeneous reactions as well as photolytic processes (see Figure 1) [*cf. Gao et al., 1997*]. We present here extensive new measurements of NO and NO<sub>y</sub> obtained in the

### Observations and box model description

The observational data set used here was acquired with instruments on board the NASA ER-2 high altitude aircraft during the Photochemistry of Ozone Loss in the Arctic Region In Summer (POLARIS) mission. The mission used deployment sites at latitudes of 37°N, 65°N, and 24°N. In the present study, data from 23 flights are used to examine NO<sub>x</sub>/NO<sub>y</sub> at high latitudes (> 60°N) in late spring, summer, and early fall periods, and in the tropics in early fall.

Measurements of NO and NO<sub>y</sub> are made with a three-channel chemiluminescence detector [*Gao et al., 1997*]. Because NO<sub>2</sub> measurements are not available for all flights, NO<sub>2</sub> values inferred from the steady state relationship (NO<sub>2</sub><sup>\*</sup>) [*Gao et al., 1997*] are used throughout for consistency. The agreement between average NO<sub>2</sub><sup>\*</sup> and observed NO<sub>2</sub> values during POLARIS is within 10% (*L. A. Del Negro et al., Comparison of modeled and observed values of NO<sub>2</sub> and JNO<sub>2</sub> during the POLARIS mission, submitted to J. Geophys. Res., 1998*). The uncertainty of the NO<sub>x</sub>/NO<sub>y</sub> measurements is estimated to be ±20%. Measured aerosol surface area (SA) densities varied between 0.5 and 1.5 μm<sup>2</sup>cm<sup>-3</sup> in the data set used here.

A photochemical steady state box model that includes only the processes shown in Figure 1 is used to calculate NO<sub>x</sub>/NO<sub>y</sub> in a sampled air parcel. The reaction set used in the model is a subset of the more comprehensive set used by *Salawitch et al. [1994]*. The model is constrained by observed values of NO, OH, ClO, O<sub>3</sub>, SA, pressure and temperature, and column O<sub>3</sub> above the aircraft [see references in *Gao et al., 1997* for instrument details]. Because NO, OH, and ClO concentrations approach zero at high solar zenith angles (SZAs), data gathered at SZA > 85° are not used in this work. The diurnal dependence of the OH radical was determined empirically and normalized here to values observed along the flight track [*Wennberg et al., 1994; T. F. Hanisco et al., unpublished data, 1999*]. Modeled ClONO<sub>2</sub> values agree with POLARIS in situ observations to within 20% (*R. M. Stimpfle et al., The coupling of ClONO<sub>2</sub>,*

<sup>1</sup>NOAA Aeronomy Laboratory, Boulder, CO.

<sup>2</sup>Cooperative Institute for Research in Environmental Sciences, University of Colorado, Boulder.

<sup>3</sup>Department of Chemistry and Biochemistry, University of Colorado, Boulder.

<sup>4</sup>The Aerospace Corporation, Los Angeles, CA.

<sup>5</sup>Division of Geology and Planetary Sciences, California Institute of Technology, Pasadena.

<sup>6</sup>Department of Chemistry, Harvard University, Cambridge, MA.

<sup>7</sup>Jet Propulsion Laboratory, California Institute of Technology, Pasadena.

<sup>8</sup>Department of Engineering, University of Denver, Denver, CO.

<sup>9</sup>NOAA Climate Monitoring and Diagnostics Laboratory, Boulder, CO.

<sup>10</sup>Department of Chemistry, University of California, Berkeley.

<sup>11</sup>Atmospheric Environment Service, Downsview, Ontario, Canada.

<sup>12</sup>NASA Ames Research Center, Moffett Field, CA.

<sup>13</sup>Atmospheric Environment Research, Inc., Cambridge, MA.

<sup>14</sup>NASA Goddard Space Flight Center, Greenbelt, MD.

Copyright 1999 by the American Geophysical Union.

Paper number 1999GL900162.  
0094-8276/99/1999GL900162\$05.00

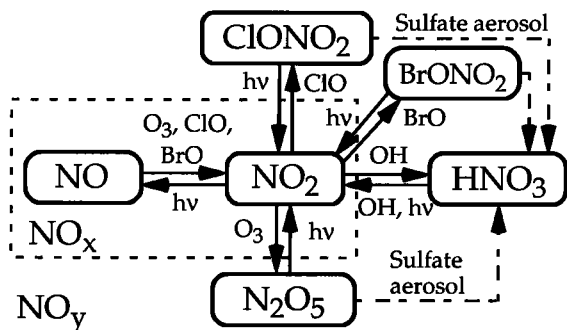


**Figure 1.** Schematic of the reaction pathways between the principal  $\text{NO}_y$  component species in the lower stratosphere. Photolysis reactions are indicated by  $h\nu$ . ‘Sulfate aerosol’ denotes heterogeneous reactions on background aerosol particles.

$\text{ClO}$ , and  $\text{NO}_2$  in the lower stratosphere from in-situ observations using the NASA ER-2 aircraft, submitted to *J. Geophys. Res.*, 1998). Model  $\text{BrO}$  values are estimated by calculating the steady state partitioning of the  $\text{Br}_y$  reservoir as estimated from organic bromine observations [Wamsley et al., 1998]. Unless otherwise noted, gas-phase rate coefficients, absorption cross sections, and reactive uptake coefficients on aerosol are taken from NASA JPL-97 recommendations [DeMore et al., 1997]. Photolysis rates are calculated using a radiation scattering model [Salawitch et al., 1994] which includes effects of overhead  $\text{O}_3$ , albedo and cloud heights. Reactive uptake coefficients of 0.1 and 0.8 are used for  $\text{N}_2\text{O}_5$  and  $\text{BrONO}_2$ , respectively. The model does not include  $\text{ClONO}_2$  hydrolysis since the reactive lifetime in sampled air parcels exceeds 100 days and thus this process has a negligible effect on  $\text{NO}_x/\text{NO}_y$  [Robinson et al., 1997]. With input parameters averaged or interpolated to 100 s intervals, the model is run to a diurnal steady state to yield a value of  $\text{NO}_y$  consistent with measured  $\text{NO}$  and rate parameters used in the model. The  $\text{NO}_x/\text{NO}_y$  deduced in this way is then compared with that inferred from  $\text{NO}_2^*$  and the measured values of  $\text{NO}$  and  $\text{NO}_y$ .

## Results

The comparison of observed and modeled  $\text{NO}_x/\text{NO}_y$ , shown in Figure 2A, includes all stratospheric data from altitudes between 17 and 20 km (50 mb < pressure < 80 mb) with temperatures greater than 204K. The approximately 200,000 s of data are distributed in latitude between  $0^\circ$  and  $90^\circ\text{N}$  (<  $40^\circ$ : 5%;  $40^\circ - 60^\circ$ : 17%; >  $60^\circ$ : 78%). In high latitude summer,  $\text{NO}_x$  reaches 3 parts per billion by volume (ppbv) with  $\text{NO}_x/\text{NO}_y$  in the range of 0.2 to 0.3. Although similar  $\text{NO}_x/\text{NO}_y$  ratios can also be found in the tropical lower stratosphere, the associated  $\text{NO}_x$  values are typically much less than 3 ppbv.

Most of the steady state model values of  $\text{NO}_x/\text{NO}_y$  fall significantly below observed values. The linear fit (forced through the origin) to the model/data regression has a slope of 0.65. The regression remains virtually unchanged if  $J_{\text{NO}_2}$  is altered to account for the small difference between  $\text{NO}_2^*$  and observed  $\text{NO}_2$  values because  $J_{\text{NO}_2}$  changes affect  $\text{NO}_2$  values on both axes in Figure 2A.

The diurnal steady state assumption is unlikely to be the cause of the observation-model discrepancy in Figure 2A. Back trajectories of the sampled air parcels were calculated using National Center for Environmental Prediction (NCEP) analyzed winds and temperatures. For each parcel, the accumulated latitude change over the previous 10 days was calculated using a weighting function inversely related to the time before aircraft sampling. When those parcels with an effective latitude

change of  $5^\circ$  or more ( $\sim 70\%$  of the data) are excluded from the data set, the regression fit to the remaining data is not significantly changed.

The model parameterization of  $\text{N}_2\text{O}_5$  hydrolysis is also unlikely to be the cause of the  $\text{NO}_x/\text{NO}_y$  discrepancy. Using NCEP back trajectories, sampled air parcels that had recently experienced nearly continuous solar illumination were identified. The acceptance criterion was an SZA of less than  $93^\circ$  for 90% of the preceding 5 day period. As solar illumination becomes continuous, the diurnal conversion of  $\text{NO}_x$  to  $\text{HNO}_3$  through  $\text{N}_2\text{O}_5$  formation and hydrolysis becomes negligible [Farman et al., 1985; Brühl et al., 1998] and hence the contribution of  $\text{N}_2\text{O}_5$  hydrolysis to  $\text{NO}_x/\text{NO}_y$  also becomes negligible. The separately averaged data sets in Figure 2A show that, overall, these selected data points are nearly indistinguishable as a group from those that experience interrupted solar illumination. In contrast to the diminished role of  $\text{N}_2\text{O}_5$  hydrolysis, the contribution of  $\text{BrONO}_2$  hydrolysis to reducing  $\text{NO}_x/\text{NO}_y$  is greatest for the continuously illuminated parcels [Randeniya et al., 1997]. However,  $\text{BrONO}_2$  hydrolysis reduces  $\text{NO}_x/\text{NO}_y$  by a maximum of only 5 - 10%. Thus, the hydrolysis reactions of  $\text{N}_2\text{O}_5$ ,  $\text{ClONO}_2$ , and  $\text{BrONO}_2$  are not effective enough in-

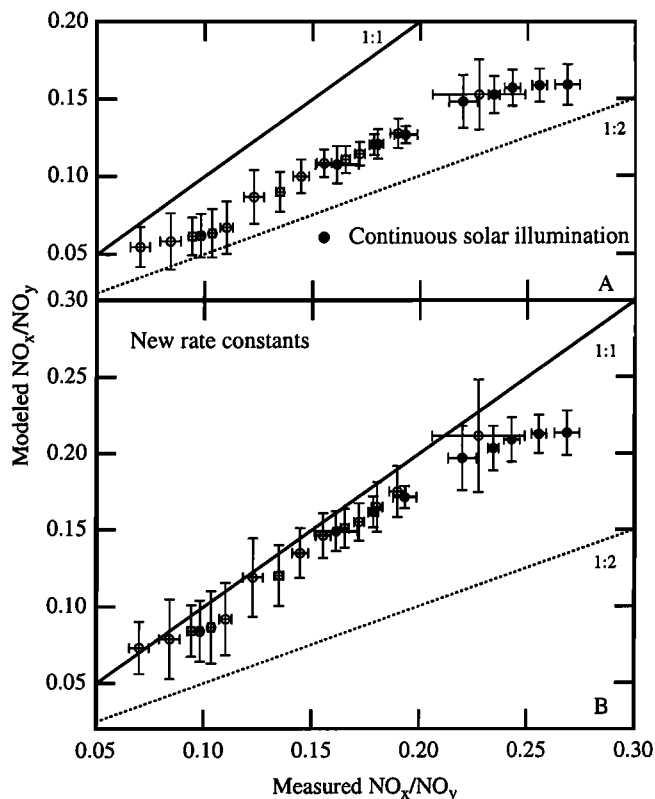


**Figure 2.** Comparison of modeled and measured values of  $\text{NO}_x/\text{NO}_y$  from POLARIS. The symbols are averages of data as grouped by increasing  $\text{NO}_x/\text{NO}_y$  value. Open symbols are averages of 80 points, each of which represented 100 s of observational data. The solid symbols are separate averages (84 points of 100 s data) for those POLARIS observations for which the sampled air parcel experienced near-continuous solar illumination for the preceding 5 days. The horizontal and vertical bars on each symbol represent the  $1-\sigma$  sample standard deviation within each group of measured and modeled values, respectively. Results are shown using the model with JPL recommended rate coefficient values (panel A) and with the Brown et al. [1999a, b] rate coefficient expressions for (1) and (2) (panel B). The solid and dashed lines represent the 1:1 and 1:2 regression slopes, respectively.

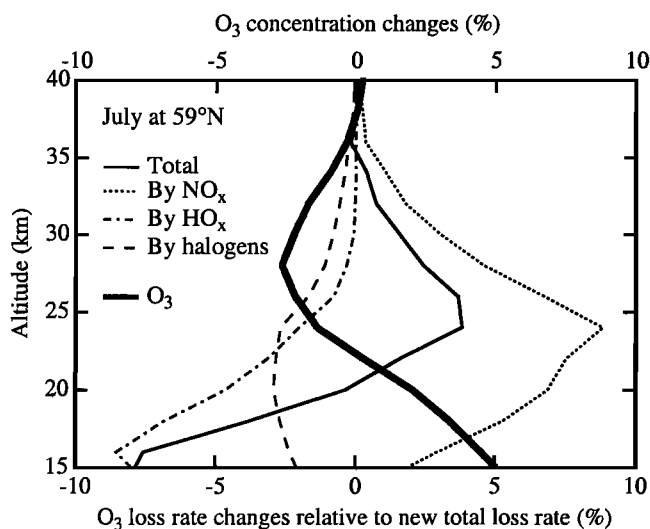
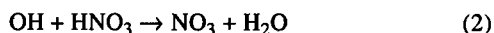
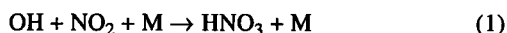


**Figure 3.** GS model results vs altitude for percentage changes in ozone, its total destruction rate, and the contributions of the NO<sub>x</sub>, HO<sub>x</sub>, and halogen catalytic cycles for average July 1990 conditions at 59°N with background aerosol conditions. The changes are those that result from using the new *Brown et al.* [1999a, b] values for  $k_1$  and  $k_2$ . The percentage changes of the catalytic cycles are shown with respect to the new total ozone loss rate. The percentage changes between the new and old values of the individual loss cycles are larger. For example, at 20 km the NO<sub>x</sub>, HO<sub>x</sub>, and halogen cycle changes are +23%, -10%, and -22%, respectively. Nearly identical results are obtained with the AER model. The representativeness of the GS model was checked by comparing the average observations at 65°N with the nearest model grid point (64°N). Noon model values of NO<sub>x</sub>/NO<sub>y</sub> are somewhat lower (< 25%) in the 15 - 20 km region at high latitudes. The longer-lived NO<sub>y</sub>, Cl<sub>y</sub>, and O<sub>3</sub> species are within 10 - 20% of the average observed values between 15 and 20 km.

dividually or collectively to cause the systematic discrepancy shown in Figure 2A.

In air parcels in which the heterogeneous hydrolysis reactions in Figure 1 do not play a strong role, NO<sub>x</sub>/NO<sub>y</sub> is primarily controlled by the gas-phase reactions:



where M is O<sub>2</sub> or N<sub>2</sub>. Only a few measurements of the rate coefficient for (1) and (2) ( $k_1$  and  $k_2$ ) are available at lower stratospheric temperatures ( $220 \pm 20\text{K}$ ) and pressures (50 - 150 mb) [DeMore *et al.*, 1997]. Donahue *et al.* [1997] first suggested that recommended values for  $k_1$  may be too high for stratospheric conditions. Recently, Dransfield *et al.* [1999] and Brown *et al.* [1999a] reported laboratory measurements of  $k_1$  for stratospheric conditions that are about 20 - 30% lower than JPL-97 values but consistent with the few previous measurements available below 298K. Brown *et al.* [1999b] also show that  $k_2$  in the lower stratosphere is higher (up to 50%) than JPL-97 values.

Incorporating the new values of  $k_1$  and  $k_2$  of Brown *et al.* [1999a, b] in the model significantly improves the overall agreement with the observations (Figure 2B). The linear fit (forced through the origin) with the new model results has a slope of 0.90. In a similar analysis using balloon observations of NO<sub>x</sub>/NO<sub>y</sub> at ER-2 altitudes and above, agreement to within

**Table 1.** Column O<sub>3</sub> change (%) at 59°N in July<sup>a</sup>

EI(SO <sub>2</sub> ) (g/kg fuel)	JPL 97 rates	Brown <i>et al.</i> rates for (1) and (2)
0	-0.5/-0.4	-0.6/-0.6
0.4 <sup>b</sup>	-1.3/-0.9	-1.0/-0.5

<sup>a</sup> AER model results for the scenario of 500 HSCT aircraft operating at Mach 2.4 near 18 km cruise altitude with an emission index (EI) of (NO<sub>x</sub>) of 5 g/kg fuel. Values are noted for both 2015 and 2050 models years as '2015/2050'. Similar values are calculated for average hemispheric O<sub>3</sub> column changes.

<sup>b</sup> With 50% conversion to small sulfate particles in the plume.

10% is achieved for a 35% reduction of  $k_1$  from JPL-97 values [Osterman *et al.*, 1999]. The Brown *et al.* values of  $k_1$  are not expected to substantially affect the Gao *et al.* [1997] results for winter polar NO<sub>y</sub> partitioning since N<sub>2</sub>O<sub>5</sub> hydrolysis is generally faster than reaction (1) under the conditions sampled. In contrast, an increase in  $k_2$  will lead to a calculated increase in NO<sub>x</sub>/NO<sub>y</sub> during winter.

An increase of the HNO<sub>3</sub> photolysis rate in (3) would also improve the observation-model comparisons in Figure 2. In the absence of changes to  $k_1$  and  $k_2$ , an increase of approximately 70% is required to yield a regression slope of 0.9. Such a large increase exceeds the reported uncertainties in the underlying measurements of the temperature dependent HNO<sub>3</sub> absorption cross section for lower stratospheric conditions [Burkholder *et al.*, 1993] or in the uncertainties associated with the radiation field calculations [Gao *et al.*, 1997; Salawitch *et al.*, 1994].

## Implications

The 2-D dynamical-chemical-radiative model of Garcia and Solomon (GS) [1994] and the AER chemistry-transport model [Weissenstein *et al.*, 1996] were used to examine the effects of the Brown *et al.* rates on O<sub>3</sub> and the principal ozone catalytic loss cycles at high latitudes in summer. The results shown in Figure 3 include altitudes between 15 and 40 km in the stratospheric ozone layer in July at 59°N to illustrate the effect of the new  $k_1$  and  $k_2$  values over a range of model temperatures and other conditions. The important features in Figure 3 are (i) that large changes in the rates that control NO<sub>x</sub>/NO<sub>y</sub> yield much smaller changes in the ozone distribution in the lower stratosphere due to the corresponding changes in HO<sub>x</sub>, ClO<sub>x</sub>, and BrO<sub>x</sub> abundances, and (ii) that the new rates result in a 'cross-over' near 20 km from an increased to a decreased value of the total O<sub>3</sub> destruction rate. Throughout most of the 15 - 40 km region, the magnitude of the NO<sub>x</sub>-catalyzed destruction increases (up to 10% near 25 km when expressed as a percentage of the new total O<sub>3</sub> destruction rate) as a direct result of higher NO<sub>x</sub>/NO<sub>y</sub> values while the contributions from the BrO<sub>x</sub>-ClO<sub>x</sub> and HO<sub>x</sub> catalytic cycles decrease because of moderation by NO<sub>x</sub>. Above 25 km, NO<sub>x</sub>/NO<sub>y</sub> approaches unity and the sensitivity of the O<sub>3</sub> loss cycles to the rate coefficient changes approaches zero. At 25 km, the net increase in O<sub>3</sub> destruction rates reaches a maximum. Because changes in  $k_2$  are largest at low temperatures and affect the abundances of both NO<sub>x</sub> and HO<sub>x</sub>, the sensitivity of the BrO<sub>x</sub>-ClO<sub>x</sub> and HO<sub>x</sub> cycles to increases in NO<sub>x</sub>/NO<sub>x</sub> is largest below 25 km and results in a net decrease in the total O<sub>3</sub> loss rate. Changes in the vertical distribution of O<sub>3</sub> due to the new rates are small (< 5%) throughout the 15 - 40 km region, consistent with the calculated changes in the O<sub>3</sub> loss rate.

The increased contribution of the NO<sub>x</sub> cycle to O<sub>3</sub> loss rates at mid and high latitudes modifies how emissions from a pro-

posed High Speed Civil Transport (HSCT) stratospheric aircraft fleet are expected to change O<sub>3</sub> in the lower stratosphere [Stolarski *et al.*, 1995]. Whether the Brown *et al.* rates will lead to a larger or smaller depletion for a particular HSCT scenario depends sensitively on the relative emissions of NO<sub>x</sub> and sulfur from an HSCT engine. The sulfur emission index (EI) and exhaust plume processes determine the SA changes of the background sulfate aerosol. As an example, Table 1 shows how the Brown *et al.* k<sub>1</sub> and k<sub>2</sub> values affect O<sub>3</sub> column amounts at 59°N in summer for two key HSCT fleet scenarios in a 2015 and 2050 atmosphere. With no sulfur emissions, the changes in the rate coefficients of k<sub>1</sub> and k<sub>2</sub> result in slightly larger O<sub>3</sub> depletion because the role of NO<sub>x</sub> in catalytic O<sub>3</sub> loss is greater than its role in moderating the HO<sub>x</sub> and halogen cycles. When sulfur is also emitted, the formation of sulfate particles in the plume and their accumulation in the atmosphere causes an increase in background SA densities. Larger SA densities reduce NO<sub>x</sub> values through N<sub>2</sub>O<sub>5</sub> hydrolysis (for both the NO<sub>x</sub> emitted by the aircraft and NO<sub>x</sub> in the background atmosphere), resulting in a decrease in the O<sub>3</sub> removal by the NO<sub>x</sub> loss cycle compared to the atmosphere without aircraft. The NO<sub>x</sub> reduction due to increased SA densities in the atmosphere increases the HO<sub>x</sub> and active halogen concentrations, resulting in increases for the corresponding O<sub>3</sub> removal cycles. The effects of increased NO<sub>x</sub> concentrations due to aircraft emission must be considered in conjunction with the effects of increased SA densities. The use of the Brown *et al.* rates in this case results in less O<sub>3</sub> depletion because more effective moderation of the HO<sub>x</sub> and halogen loss cycles by aircraft-emitted NO<sub>x</sub> partially mitigates the effect of aerosol changes.

### Concluding remarks

The in situ aircraft observations presented here represent a large new data set with which to examine NO<sub>x</sub>/NO<sub>y</sub> over a wide range of latitude and season in the lower stratosphere. Representative box model calculations systematically underpredict the observed ratio by about 40%. Because the discrepancy remains in air parcels with continuous solar exposure, the parameterization of the N<sub>2</sub>O<sub>5</sub> hydrolysis reaction is unlikely to be the cause. The use of recent laboratory results for the OH + NO<sub>2</sub> and OH + HNO<sub>3</sub> reaction rate coefficients from Brown *et al.* [1999a, b] significantly improves the comparison of measured and modeled NO<sub>x</sub>/NO<sub>y</sub> for most sampled air parcels. The effect of the rate changes and associated NO<sub>x</sub> increases on O<sub>3</sub> concentrations calculated in 2-D models is small (< 5%) throughout most of the lower stratosphere because of the interdependence of the NO<sub>x</sub>, BrO<sub>x</sub>-ClO<sub>x</sub>, and HO<sub>x</sub> catalytic loss cycles.

**Acknowledgments.** We thank the pilots and ground crew of the NASA ER-2 aircraft. This work is supported by the NASA Upper Atmospheric Research Program and the Atmospheric Effects of Aviation Project.

### References

- Brown, S. S., R. K. Talukdar, and A. R. Ravishankara, Rate constants for the reaction OH + NO<sub>2</sub> + M → HNO<sub>3</sub> + M under atmospheric conditions, *Chem. Phys. Lett.*, **299**, 277-284, 1999a.
- Brown, S. S., R. K. Talukdar, and A. R. Ravishankara, Reconsideration of the rate constant for the reaction of hydroxyl radicals with nitric acid, *J. Phys. Chem.*, in press, 1999b.
- Brihl, C., P. J. Crutzen, and J.-U. Grob, High-latitude, summertime NO<sub>x</sub> activation and seasonal ozone decline in the lower stratosphere: Model calculations based on observations by HALOE on UARS, *J. Geophys. Res.*, **103**, 3587-3597, 1998.
- Burkholder, J. B., R. K. Talukdar, A. R. Ravishankara, and S. Solomon, Temperature dependence of the HNO<sub>3</sub> UV absorption cross sections, *J. Geophys. Res.*, **98**, 22937-22948, 1993.

- DeMore, W. B., *et al.*, Chemical kinetics and photochemical data for use in stratospheric modeling, *JPL Publ. 97-4*, Jet Propul. Lab., Pasadena, Calif., 1997.
- Donahue, N. M., M. Dubey, R. Mohrschladt, K. L. Demerjian, and J. G. Anderson, A high pressure flow study of the reactions OH + NO<sub>x</sub> → HONO<sub>x</sub>: Errors in the falloff region, *J. Geophys. Res.*, **102**, 6159-6168, 1997.
- Dransfield, T. J., K. K. Perkins, N. M. Donahue, J. G. Anderson, M. M. Sprengnether, and K. L. Demerjian, Temperature and pressure dependent kinetics of the gas-phase reaction of the hydroxyl radical with nitrogen dioxide, *Geophys. Res. Lett.*, in press, 1999.
- Fahey, D. W., *et al.*, In situ measurements constraining the role of sulfate aerosols in mid-latitude ozone depletion, *Science*, **363**, 509-514, 1993.
- Farman, J. C., R. J. Murgatroyd, A. M. Silnickas, and B. A. Thrush, Ozone photochemistry in the Antarctic stratosphere in summer, *Q. J. Royal Met. Soc.*, **111**, 1013-1028, 1985.
- Garcia, R. R. and S. Solomon, A new numerical model of the middle atmosphere: 2. Ozone and related species, *J. Geophys. Res.*, **99**, 12937-12951, 1994.
- Gao, R. S., *et al.*, Partitioning of the reactive nitrogen reservoir in the lower stratosphere of the southern hemisphere: Observations and modeling, *J. Geophys. Res.*, **102**, 3935-3949, 1997.
- Osterman, G. B., B. Sen, G. C. Toon, R. J. Salawitch, J. J. Margitan, J.-F. Blavier, D. W. Fahey, and R. S. Gao, Partitioning of NO<sub>y</sub> species in the summer Arctic stratosphere, *Geophys. Res. Lett.*, this issue, 1999.
- Randeniya, L. K., P. F. Vohralik, I. C. Plumb, and K. R. Ryan, Heterogeneous BrONO<sub>2</sub> hydrolysis: Effect on NO<sub>2</sub> columns and ozone at high latitude in summer, *J. Geophys. Res.*, **102**, 23,543-23,557, 1997.
- Robinson, G. N., D. R. Worsnop, J. T. Jayne, C. E. Kolb, and P. Davidovits, Heterogeneous uptake of ClONO<sub>2</sub> and N<sub>2</sub>O<sub>5</sub> by sulfuric acid solutions, *J. Geophys. Res.*, **102**, 3583-3601, 1997.
- Salawitch, R. J., *et al.*, The diurnal variation of hydrogen, nitrogen, and chlorine radicals: Implications for the heterogeneous production of HNO<sub>2</sub>, *Geophys. Res. Lett.*, **21**, 2551-2554, 1994.
- Stolarski, R. S., *et al.*, 1995 Scientific assessment of the atmospheric effects of stratospheric aircraft, *NASA Ref. Publ. 1381*, Washington, D.C., 1995.
- Wamsley, P. R. *et al.*, Distribution of halon-1211 in the upper troposphere and lower stratosphere and the 1994 total bromine budget, *J. Geophys. Res.*, **103**, 1513-1526, 1998.
- Weisenstein, D. K., *et al.*, Potential impact of SO<sub>2</sub> emissions from stratospheric aircraft on ozone, *Geophys. Res. Lett.*, **23**, 161-164, 1996.
- Wennberg, P. O., *et al.*, Removal of stratospheric O<sub>3</sub> by radicals: In situ measurements of OH, HO<sub>2</sub>, NO<sub>2</sub>, ClO, and BrO, *Science*, **266**, 398-404, 1994.

S. S. Brown, S. G. Donnelly, D. W. Fahey, R. S. Gao, J. A. Neuman, R. W. Portmann, M. J. Proffitt, and E. Teverovski, NOAA Aeronomy Laboratory, Boulder, CO, and Cooperative Institute for Research in Environmental Sciences (CIRES), University of Colorado, Boulder.

T. P. Bui, NASA Ames Research Center, Moffett Field, CA.

R. C. Cohen, Department of Chemistry, University of California, Berkeley.

L. A. Del Negro, A. R. Ravishankara, NOAA Aeronomy Laboratory, Boulder, CO; CIRES; Department of Chemistry and Biochemistry, University of Colorado, Boulder.

J. W. Elkins, NOAA Climate Monitoring and Diagnostics Laboratory, Boulder, CO.

T. F. Hanisco, E. J. Lanzendorf, R. M. Stimpfle, Department of Chemistry, Harvard University, Cambridge, MA.

E. R. Keim, The Aerospace Corporation, Los Angeles, CA.

M. K. W. Ko, D. K. Weisenstein, Atmospheric Environment Research, Inc., Cambridge, MA.

J. J. Margitan, R. J. Salawitch, Jet Propulsion Laboratory, California Institute of Technology, Pasadena.

C. T. McElroy, Atmospheric Environment Service, Downsview, Ontario, Canada.

P. A. Newman, NASA Goddard Space Flight Center, Greenbelt, MD.

P. O. Wennberg, California Institute of Technology, Pasadena.

J. C. Wilson, Department of Engineering, University of Denver, Denver, CO.

(Received November 24, 1998; revised February 18, 1999; accepted February 22, 1999.)